Naveen Pathivada[1], Gopi Mamidi[2], Amancharla Indira Priyadarsini[3], Gunduluru Swathi[4]*

[1]Lecturer in Chemistry, Government Degree College (Autonomous), Nagari, Andhra Pradesh, India, [2]Lecturer in Chemistry, Dr. V.S.K. Government Degree College, Visakhapatnam, Andhra Pradesh, India, [3]Lecturer in Botany, Government Degree College (Autonomous), Nagari, Andhra Pradesh, India, [4]Lecturer in Zoology, Government Degree College (Autonomous), Nagari, Andhra Pradesh, India

Scientific paper
ISSN 0351-9465, E-ISSN 2466-2585
https://doi.org/10.62638/ZasMat1843

Zastita Materijala 67 ()
(2026)

Comparative green synthesis of silver nanoparticles using seed and pod extracts of *amomum aromaticum* and their biological evaluation

ABSTRACT

Silver nanoparticles (AgNPs) synthesized through plant-mediated routes have attracted considerable attention for biomedical applications due to their eco-friendly preparation, cost-effectiveness, and functional properties. However, most previous studies have employed either a single plant organ or whole-plant extracts, with limited investigation of how different organs of the same species may influence nanoparticle formation and biologicalperformance. In the present study, aqueous seed and pod extracts of Amomum aromaticum were comparatively used for the green synthesis of AgNPs under controlled near-neutral conditions (pH 6.0 ± 0.2). The synthesized nanoparticles were characterized using UV–Visible spectroscopy, FTIR, XRD, TEM, DLS, EDX, and zeta potential analysis. The results confirmed the formation of stable and crystalline AgNPs, with clear extract-dependent differences in physicochemical characteristics. Seed-derived AgNPs were smaller (15–20 nm) and exhibited higher colloidal stability (−25.4 ± 1.2 mV), whereas pod-derived AgNPs were relatively larger (25–30 nm) and displayed distinct surface characteristics. Biological evaluation indicated that Seed-AgNPs showed comparatively stronger antibacterial activity against Staphylococcus aureus and Escherichia coli, while Pod-AgNPs demonstrated enhanced antioxidant activity (81 ± 2.1%) and improved wound closure (78 ± 3.1% within 24 h) in an in vitro assay. The novelty of this study lies in its controlled organ-specific comparison, demonstrating that different parts of the same plant can direct nanoparticle characteristics and functional responses under identical synthesis conditions. Overall, the findings indicate that plant organ selection can significantly influence the physicochemical properties and observed biological performance of green-synthesized agnps. further studies involving detailed phytochemical profiling and mechanistic validation are required to establish direct causal relationships.

Keywords: *Green synthesis; silver nanoparticles; amomum aromaticum; plant-mediated synthesis; antibacterial activity; antioxidant activity; wound healing; nanobiotechnology*

1. INTRODUCTION

Nanotechnology has contributed significantly to the development of advanced materials for biomedical and environmental applications by enabling control over matter at the nanoscale. Among metallic nanomaterials, silver nanoparticles (AgNPs) have been widely investigated due to their distinctive optical properties, high surface reactivity, and broad-spectrum antimicrobial activity [1–3]. These properties have supported their use in wound dressings, antibacterial coatings, antioxidant systems, and drug delivery platforms [4–6].

However, conventional chemical and physical methods for AgNP synthesis often involve toxic reducing agents, elevated temperatures, or high energy input, which may limit their applicability in biological systems and raise environmental concerns [7]. As a result, green synthesis approaches—particularly plant-mediated methods—have gained increasing attention as more sustainable alternatives. Plant extracts contain a variety of phytochemicals capable of reducing Ag^+ ions to Ag^0 while also contributing to nanoparticle stabilization, thereby minimizing the use of hazardous reagents and potentially improving biocompatibility [8–10].

Despite extensive research on plant-mediated synthesis of AgNPs, most studies rely on either whole-plant extracts or a single plant organ, such as leaves or fruits [11–13]. This approach often assumes that different parts of the same plant

*Corresponding author: Naveen Pathivada
E- mail: naveen.sklm@gmail.com
Paper received: 29.04.2026.
Paper corrected: 03.05.2026.
Paper accepted: 06.05.2026.

contribute similarly to nanoparticle formation. In practice, however, plants exhibit organ-specific metabolic specialization, and the composition of secondary metabolites can vary considerably between seeds, pods, leaves, and roots [14,15]. Such variation may influence nanoparticle nucleation, growth kinetics, and surface chemistry. Nevertheless, systematic investigations of intra-species, organ-level differences under controlled synthesis conditions remain limited, and only a few studies have attempted to relate these differences to variations in biological activity [16,17]. Consequently, the role of plant organ selection as an experimental factor in green nanoparticle synthesis remains insufficiently explored. *Amomumaromaticum*Roxb. (Bengal cardamom), belonging to the family Zingiberaceae, is a medicinal plant traditionally used for its antimicrobial, anti-inflammatory, and digestive properties [18,19]. Phytochemical studies suggest that different organs of this plant possess distinct chemical profiles. The seeds are reported to contain higher levels of flavonoids and related polyphenols, which can act as electron donors and may facilitate metal ion reduction [20]. In contrast, the pods contain relatively higher levels of phenolic acids and tannins, compounds associated with antioxidant activity and potential roles in wound-healing processes [21,22]. This inherent phytochemical variation within a single plant species provides a suitable basis for examining whether organ-specific extracts can influence nanoparticle formation and associated biological responses when synthesis conditions are held constant.In this study, silver nanoparticles were synthesized separately using aqueous seed and pod extracts of *A. aromaticum* under controlled near-neutral conditions.

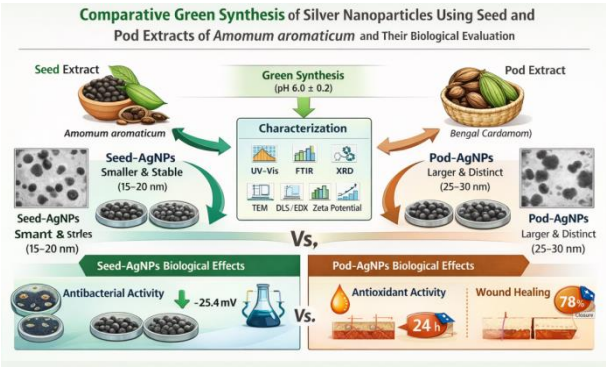

The resulting nanoparticles were characterized using UV–Vis spectroscopy, FTIR, XRD, TEM, DLS, EDX, and zeta potential analysis to evaluate differences in size, morphology, and stability. Biological activity was assessed through antioxidant, antibacterial, cytotoxicity, biofilm inhibition, and in vitro wound-healing assays with appropriate controls and statistical analysis [23–26]. The study focuses on identifying observable differences associated with extract type under identical experimental conditions. While possible links between phytochemical composition and nanoparticle behavior are discussed, these are inferred based on spectroscopic evidence and literature reports rather than direct phytochemical quantification. Therefore, the findings should be interpreted as indicative rather than mechanistically conclusive.

Novelty of the Present Study

The novelty of this work lies in its organ-specific, intra-species approach to green synthesis of silver nanoparticles, in contrast to the more commonly reported use of a single plant organ or cross-species comparisons. While plant-mediated synthesis of AgNPs is well established, systematic evaluation of how different organs of the same plant influence nanoparticle characteristics and associated biological responses remains relatively limited. In the present study, seed and pod extracts of *Amomum aromaticum* were employed under identical synthesis conditions, allowing the effect of extract type to be examined while minimizing variations arising from reaction parameters such as pH, temperature, and precursor concentration. The results indicate that the choice of plant organ can influence nanoparticle size, surface characteristics, and colloidal stability. Seed-derived AgNPs were observed to exhibit smaller particle size and higher colloidal stability, along with comparatively stronger antibacterial activity, whereas pod-derived AgNPs showed relatively higher antioxidant activity and improved wound closure in an in vitro assay. These differences may be associated with variations in phytochemical composition between the two extracts, as inferred from FTIR analysis and supported by literature reports. Overall, the findings suggest that organ-specific extract selection can influence the properties and observed biological performance of green-synthesized AgNPs under controlled conditions. However, the proposed role of specific phytochemicals remains to be validated through detailed compositional analysis. Thus, the study provides a controlled experimental perspective on intra-species variability in plant-mediated nanoparticle synthesis, rather than a definitive mechanistic framework.

2. MATERIALS AND METHODS

2.1. Chemicals and Reagents

Silver nitrate ($AgNO_3$, ≥99.9% purity) was obtained from an analytical-grade supplier and used without further purification. All solutions were prepared using double-distilled water. Reagents required for antioxidant, antibacterial, cytotoxicity,

biofilm inhibition, and wound-healing assays were of analytical grade and used as received. Experimental procedures were adapted from established protocols reported in the literature [4,6].

2.2. Plant Material Collection and Authentication

Fresh fruits of *Amomumaromaticum*Roxb. (Bengal cardamom) were collected from Tirupati, Andhra Pradesh, India. Botanical authentication was carried out by Dr. A. Indira Priyadarsini, Department of Botany, Government Degree College (Autonomous), Nagari. A voucher specimen (Voucher No. AAR-2025-01) was deposited in the institutional herbarium for future reference. The collected fruits were washed thoroughly with distilled water, manually separated into seeds and pods, and dried in a hot-air oven at 50 °C until constant weight was achieved to minimize phytochemical degradation.

2.3. Preparation of Seed and Pod Extracts

Dried seed and pod materials were ground separately into fine powders using a sterile mechanical grinder. For aqueous extraction, 5 g of each powdered sample was boiled in 100 mL of distilled water for 20 min. The extracts were cooled to room temperature and filtered through Whatman No. 1 filter paper to remove particulate matter. The resulting extracts corresponded to an approximate concentration of 50 mg mL^{-1} (dry weight basis) and were stored at 4 °C until further use. These extracts functioned as both reducing and stabilizing agents during nanoparticle synthesis [1,8,9].

2.4. Phytochemical Quantification of Seed and Pod Extracts

To better understand the compositional differences between the seed and pod extracts of Amomum aromaticum, preliminary phytochemical quantification was carried out using standard spectrophotometric methods. Total phenolic content (TPC) was determined using the Folin–Ciocalteu method and expressed as mg gallic acid equivalents (GAE) per g dry extract [24]. Total flavonoid content (TFC) was estimated using the aluminium chloride colorimetric assay and expressed as mg quercetin equivalents (QE) per g dry extract [25]. Condensed tannin content was measured using a vanillin-based spectrophotometric method and expressed as mg catechin equivalents (CE) per g dry extract [26]. All measurements were performed in triplicate, and results are presented as mean ± standard deviation.

2.5. Green Synthesis of Silver Nanoparticles

A freshly prepared 1 mM aqueous $AgNO_3$ solution was mixed with each plant extract in a 1:1 (v/v) ratio under ambient conditions. The pH of the reaction mixture was adjusted to 6.0 ± 0.2 using 0.1 M NaOH or HCl and monitored using a calibrated digital pH meter. Preliminary experiments conducted across a pH range of 4–8 indicated that near-neutral conditions resulted in stable colloidal suspensions with well-defined surface plasmon resonance bands, consistent with previous reports on plant-mediated AgNP synthesis. The reaction mixtures were incubated at 25 ± 2 °C without stirring. Formation of AgNPs was initially indicated by a visible color change from pale yellow to reddish brown within approximately 30 mi. After completion of the reaction, the nanoparticle suspensions were centrifuged at 12,000 rpm for 15 min at room temperature to separate the synthesized AgNPs. The collected pellets were washed three times with double-distilled water to remove unreacted silver ions and loosely bound phytochemical residues, followed by one additional wash with ethanol to facilitate purification. The purified nanoparticles were then re-dispersed in distilled water or dried in a hot-air oven at 50 °C for 12 h, depending on the subsequent characterization or biological assay requirements. The dried samples were stored in sterile airtight containers at room temperature until further use.

2.6. Characterization of Silver Nanoparticles

2.6.1. UV–Visible Spectroscopy

UV–Visible absorption spectra were recorded in the range of 300–600 nm using a UV–Vis spectrophotometer (Shimadzu UV-1800, Japan) to confirm the surface plasmon resonance of the synthesized AgNPs [13].

2.6.2. Fourier Transform Infrared (FTIR) Spectroscopy

FTIR spectra were recorded in the range of 4000–400 cm^{-1} using an FTIR spectrometer (PerkinElmer Spectrum Two, USA) with the KBr pellet method to identify functional groups involved in Ag^{+} reduction and nanoparticle stabilization [9].

2.6.3. X-ray Diffraction (XRD)

Crystalline structure and phase purity were analyzed using an X-ray diffractometer (RigakuMiniFlex 600, Japan) equipped with Cu Kα radiation (λ = 1.5406 Å), scanning over a 2θ range of 10°–80° [13].

2.6.4. Transmission Electron Microscopy (TEM)

Particle morphology and size distribution were examined using transmission electron microscopy (JEOL JEM-2100, Japan). Particle size was estimated by measuring multiple nanoparticles from representative micrographs [13].

2.6.5. Dynamic Light Scattering (DLS) and Zeta Potential

Hydrodynamic diameter, polydispersity index (PDI), and zeta potential were measured using a

particle size analyzer (Malvern Zetasizer Nano ZS, UK) to assess colloidal stability [14].

2.6.6. Energy-Dispersive X-ray Spectroscopy (EDX)

Elemental composition of the nanoparticles was confirmed using energy-dispersive X-ray spectroscopy attached to the electron microscope (Oxford Instruments X-Max, UK) [13].

2.7. Biological Activity Evaluation

All experiments were performed in triplicate (n = 3), and results are presented as mean ± standard deviation. All in vitro experiments were conducted following standard laboratory safety guidelines.

2.7.1. Antioxidant Activity

Free radical scavenging activity was evaluated using the DPPH assay following standard procedures. Results were expressed as percentage radical scavenging activity [12,18].

2.7.2. Antibacterial Activity

Antibacterial activity was assessed using the agar well diffusion method against *Staphylococcus aureus* and *Escherichia coli*. AgNP concentrations ranged from 50 to 200 μg mL^{-1}. Ciprofloxacin (10 μg mL^{-1}) and distilled water were used as positive and negative controls, respectively [4,13].

2.7.3. Cytotoxicity Assay

Cytotoxicity was evaluated using the MTT assay on human fibroblast cell lines following established protocols. Cell viability was expressed as a percentage relative to untreated controls [5].

2.7.4. Biofilm Inhibition Assay

Biofilm inhibition was quantified using the crystal violet staining method following reported procedures [21].

2.7.5. In Vitro Wound-Healing (Scratch) Assay

Cell migration and wound closure were assessed using an in vitro scratch assay on confluent fibroblast monolayers. Wound closure percentage was calculated after 24 h of incubation [15,22].

2.8. Statistical Analysis

All experiments were performed in triplicate (n = 3), and results are presented as mean ± standard deviation. Statistical analysis was carried out using one-way analysis of variance (ANOVA) followed by Tukey's multiple comparison post-hoc test. Differences were considered statistically significant at $p < 0.05$. Effect size was additionally estimated using eta squared (η^2) for ANOVA and Cohen's d for pairwise comparisons, where appropriate. Statistical analyses were performed using GraphPad Prism (GraphPad Software Inc., USA).

Table 1. Physicochemical Characteristics and Biological Activities of Seed- and Pod-Derived AgNPs

Category	Parameter	Unit	Seed-AgNPs	Pod-AgNPs
Physicochemical Properties	UV–Vis λ_{max}	nm	432 ± 2	445 ± 3
	TEM size	nm	15–20	25–30
	DLS mean size	nm	22.5 ± 1.6	31.8 ± 2.1
	Polydispersity index (PDI)	—	0.28	0.32
	Zeta potential	mV	−25.4 ± 1.2	−18.1 ± 0.9
	Crystallite size (XRD)	nm	18.3	27.4
	Dominant capping groups	—	Flavonoids / amide	Phenolics / tannins
	Morphology	—	Spherical	Semi-spherical
Elemental Composition (EDX)	Ag	wt %	85.6	82.4
	O	wt %	7.9	9.8
	C	wt %	6.5	7.8
Biological Activities	DPPH scavenging	%	67 ± 2.4	81 ± 2.1
	S. aureus ZOI	mm	18.2 ± 1.3	14.1 ± 0.9
	E. coli ZOI	mm	16.7 ± 1.1	12.9 ± 1.0
	Cell viability (100 μg/mL)	%	82 ± 3	85 ± 4
	Wound closure (24 h)	%	55 ± 2.8	78 ± 3.1
	Biofilm inhibition	%	49 ± 2.2	51 ± 2.5

3. RESULTS AND DISCUSSION

3.1. Formation and optical characteristics of AgNPs

The formation of silver nanoparticles using seed and pod extracts of *Amomum aromaticum* was first observed through a visible color change of the reaction mixture from pale yellow to reddish brown within approximately 30 min. This change is commonly associated with surface plasmon resonance (SPR), which occurs due to the interaction of light with conduction electrons in metallic nanoparticles [2,13].

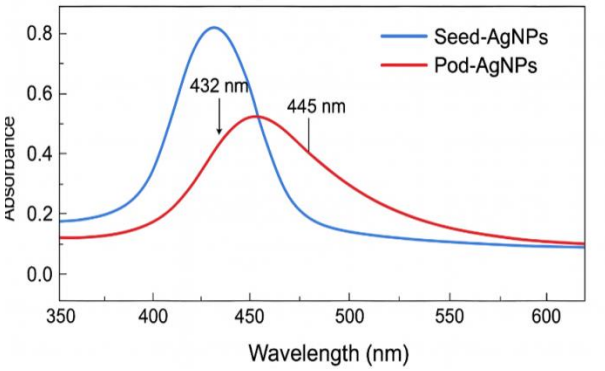

Figure 1. UV–Visible absorption spectra of silver nanoparticles synthesized using seed and pod extracts of A. aromaticum. Distinct surface plasmon resonance (SPR) peaks are observed at 432 nm for Seed-AgNPs and 445 nm for Pod-AgNPs, confirming nanoparticle formation. The observed shift in SPR peak position may be associated with differences in particle size and/or the surrounding dielectric environment

The UV–Visible spectra (Figure 1) provided further confirmation of nanoparticle formation. Seed-derived AgNPs showed a clear SPR peak at 432 ± 2 nm, while pod-derived AgNPs exhibited a slightly red-shifted peak at 445 ± 3 nm. Such a shift is generally linked to differences in particle size or changes in the surrounding dielectric environment [13,14]. The SPR band for Seed-AgNPs appeared relatively sharp, suggesting a more uniform size distribution. In contrast, the broader peak observed for Pod-AgNPs indicates a comparatively wider size distribution. These differences may be related to variations in the composition of the seed and pod extracts, which could influence nanoparticle formation and growth behavior.

3.2. Role of phytochemicals in reduction and stabilization

FTIR analysis (Figure 2) was carried out to examine the functional groups potentially involved in the reduction of Ag^+ ions and stabilization of the synthesized nanoparticles. A broad absorption band observed around 3420 cm^{-1} can be attributed to O–H stretching vibrations, which are commonly associated with hydroxyl groups present in flavonoids and phenolic compounds [9,18]. The peak near 1634 cm^{-1} corresponds to C=O stretching of amide or conjugated carbonyl groups, while bands around 1385 cm^{-1} may be assigned to C–N stretching or aromatic C=C vibrations. Some differences were observed between the spectra of Seed- and Pod-derived AgNPs. The seed-derived nanoparticles showed relatively stronger absorption features associated with flavonoid-type compounds, whereas the pod-derived samples exhibited more pronounced signals that may be linked to phenolic acids and tannins.

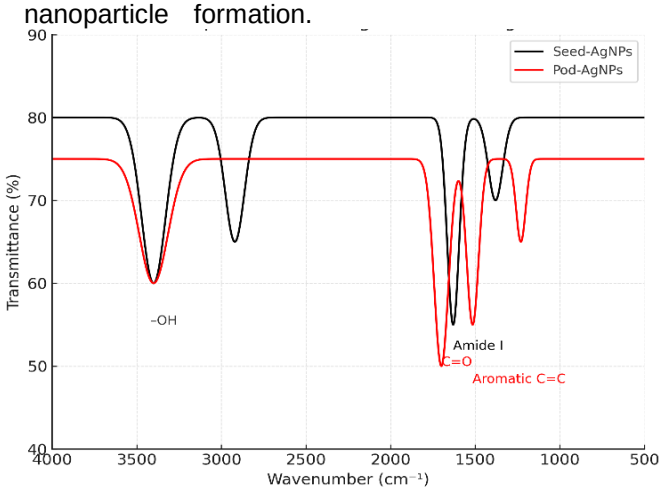

Figure 2. FTIR spectra of seed and pod extracts and their corresponding AgNPs. Major absorption bands are observed around 3420 cm^{-1} (O–H stretching), 1634 cm^{-1} (C=O stretching), and 1385 cm^{-1} (C–N and/or aromatic C=C vibrations). These bands are consistent with the presence of functional groups associated with flavonoids and phenolic compounds, which may be involved in nanoparticle reduction and surface stabilization

These variations are consistent with previously reported differences in phytochemical composition between plant organs. Flavonoids are known to act as electron donors and may contribute to the reduction of Ag^+ ions, potentially leading to faster nucleation and the formation of smaller nanoparticles [18,20]. On the other hand, phenolic acids and tannins, which contain multiple hydroxyl groups, may provide effective surface capping, contributing to nanoparticle stabilization and possibly influencing antioxidant behavior [12,22]. Because FTIR primarily provides qualitative information, additional phytochemical quantification was performed to further compare the two extracts. As presented in Table 2, the seed extract contained significantly higher flavonoid content, whereas the pod extract showed higher levels of total phenolics and condensed tannins. These findings provide quantitative support for the compositional differences inferred from the FTIR spectra. It should be noted that the proposed relationships between phytochemical composition and nanoparticle behaviour remain interpretative rather than definitive. Nevertheless, the combined FTIR and quantitative phytochemical results suggest that extract composition may influence nanoparticle formation, surface stabilization, and the observed biological responses.

Table 2. Quantitative Phytochemical Composition of Seed and Pod Extracts of Amomum aromaticum

Parameter	Unit	Seed Extract	Pod Extract	*p*-value
Total Phenolic Content (TPC)	mg GAE/g dry extract	42.6 ± 1.8	59.4 ± 2.1	*<0.01*
Total Flavonoid Content (TFC)	mg QE/g dry extract	37.8 ± 1.5	25.3 ± 1.4	*<0.01*
Condensed Tannin Content	mg CE/g dry extract	19.4 ± 1.0	34.1 ± 1.7	*<0.01*

The phytochemical analysis revealed clear organ-specific differences between the two extracts. Seed extract contained significantly higher flavonoid content, whereas pod extract showed higher levels of total phenolics and condensed tannins ($p< 0.01$). These differences may contribute to the distinct nanoparticle characteristics and biological responses observed in the present study.

3.3. Quantitative Phytochemical Composition of Seed and Pod Extracts

To further examine the compositional differences suggested by FTIR analysis, quantitative phytochemical assays were performed for the seed and pod extracts of Amomum aromaticum. The results (Table 2) revealed statistically significant organ-specific variation in the measured phytochemical classes. The seed extract showed a significantly higher total flavonoid content (37.8 ± 1.5 mg QE/g dry extract) compared with the pod extract (25.3 ± 1.4 mg QE/g dry extract; $p< 0.01$). In contrast, the pod extract contained higher levels of total phenolics (59.4 ± 2.1 mg GAE/g dry extract) and condensed tannins (34.1 ± 1.7 mg CE/g dry extract) than the seed extract (42.6 ± 1.8 and 19.4 ± 1.0 mg CE/g dry extract, respectively; $p< 0.01$).These findings are consistent with the FTIR observations and may help explain the differences observed during nanoparticle formation and biological performance. Higher flavonoid content in the seed extract may favour faster reduction of Ag^+ ions and increased nucleation, contributing to the formation of comparatively smaller nanoparticles [18,20]. Conversely, the higher phenolic and tannin content of the pod extract may enhance surface capping and free-radical scavenging behaviour, which could be associated with the stronger antioxidant and wound-healing responses observed for Pod-AgNPs [12,22]. Although these relationships are based on correlation rather than direct mechanistic evidence, the quantitative data provide additional support for the role of plant organ selection in influencing green nanoparticle synthesis outcomes [11,23].

3.4. Crystallinity and phase confirmation

XRD patterns of Seed- and Pod-derived AgNPs (Figure 3) showed characteristic diffraction peaks corresponding to the (111), (200), (220), and (311) planes of face-centered cubic (FCC) metallic silver (JCPDS No. 04-0783) [13]. The absence of additional peaks suggests that the synthesized nanoparticles are predominantly crystalline silver with no detectable impurity phases. A difference in peak intensity and sharpness was observed between the two samples. Seed-derived AgNPs exhibited relatively sharper and more intense

peaks compared to Pod-derived AgNPs, indicating higher crystallinity and smaller crystallite size. The average crystallite sizes, estimated using the Scherrer equation, were approximately 18 nm for Seed-AgNPs and 27 nm for Pod-AgNPs. Smaller crystallite size is often associated with faster nucleation processes during nanoparticle formation. In this context, the relatively smaller size observed for Seed-AgNPs may be related to differences in extract composition, which could influence reduction kinetics and particle growth behavior [18,19].

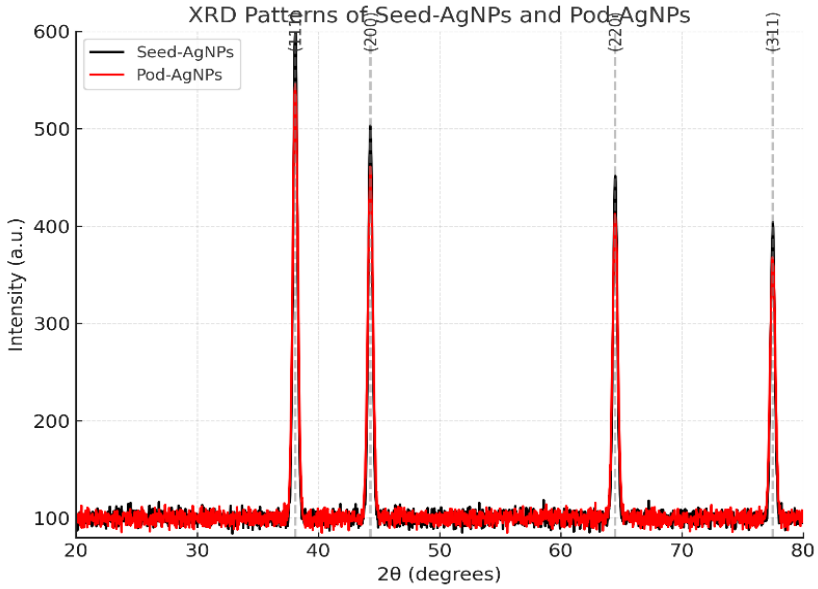

Figure 3. X-ray diffraction (XRD) patterns of Seed-AgNPs and Pod-AgNPs. Characteristic Bragg reflections corresponding to the (111), (200), (220), and (311) planes are consistent with the face-centered cubic (FCC) structure of metallic silver (JCPDS No. 04-0783). The relatively sharper peaks observed for Seed-AgNPs suggest a smaller crystallite size (approximately 18 nm) compared to Pod-AgNPs

3.5. Morphology and size distribution

TEM analysis (Figure 4) provided direct visualization of the morphology and size distribution of the synthesized nanoparticles. Seed-derived AgNPs were predominantly spherical, well dispersed, and ranged between 15–20 nm.

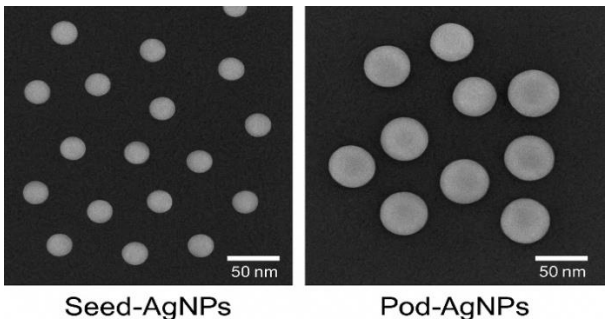

Figure 4. Transmission electron microscopy (TEM) images and corresponding particle size distributions of Seed- and Pod-derived AgNPs. Seed-AgNPs appear predominantly spherical and well dispersed, with particle sizes in the range of 15–20 nm. In contrast, Pod-AgNPs show semi-spherical morphology with a broader size range of 25–30 nm and slight aggregation

In contrast, Pod-derived AgNPs showed semi-spherical morphology with a broader size range of 25–30 nm and minor aggregation. These differences in morphology and size distribution may be related to variations in extract composition, which can influence nanoparticle nucleation and growth behavior. In general, faster nucleation processes tend to limit particle growth, leading to smaller and more uniform nanoparticles, whereas stronger surface capping can influence growth dynamics and particle dispersion [18,19].

DLS measurements (Figure 5) further supported the TEM observations. Seed-AgNPs exhibited a smaller hydrodynamic diameter (22.5 ± 1.6 nm) compared to Pod-AgNPs (31.8 ± 2.1 nm). The slightly larger sizes obtained from DLS relative to TEM are expected, as DLS measures the hydrodynamic diameter, which includes the solvation layer and surface-bound organic molecules [14].

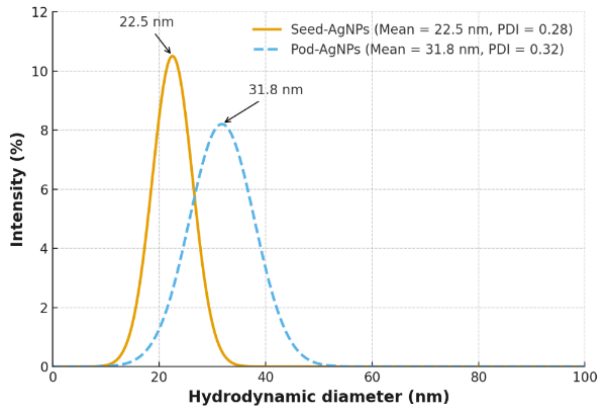

Figure 5. Dynamic light scattering (DLS) analysis of Seed- and Pod-derived AgNPs. The hydrodynamic diameter distributions show mean particle sizes of 22.5 nm for Seed-AgNPs and 31.8 nm for Pod-AgNPs, with corresponding polydispersity indices (PDI) of 0.28 and 0.32. These values suggest a relatively narrow size distribution and indicate moderate colloidal stability

3.6. Elemental composition and colloidal stability

EDX spectra (Figure 6) confirmed the presence of elemental silver, indicated by a strong signal at approximately 3 keV, along with minor peaks corresponding to carbon and oxygen. These additional elements are likely associated with organic residues from the plant extracts adsorbed on the nanoparticle surface, suggesting the presence of phytochemical capping [9,13].

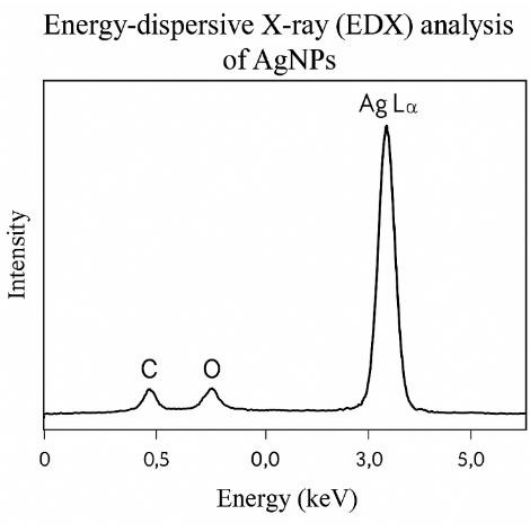

Figure 6. Energy-dispersive X-ray (EDX) spectrum of AgNPs. A prominent signal observed at approximately 3 keV is characteristic of elemental silver. Minor peaks corresponding to carbon (~0.28 keV) and oxygen (~0.52 keV) are also present, which may be associated with organic residues from plant-derived capping agents

Zeta potential analysis (Figure 7) showed values of −25.4 ± 1.2 mV for Seed-AgNPs and −18.1 ± 0.9 mV for Pod-AgNPs. In general, zeta potential values greater than ±20 mV are considered indicative of reasonably stable colloidal systems due to electrostatic repulsion between particles [14].Based on these values, Seed-AgNPs appear to exhibit comparatively higher colloidal stability than Pod-AgNPs. This difference in stability may influence nanoparticle dispersion and interaction behavior in solution, which could contribute to variations observed in their biological activity.

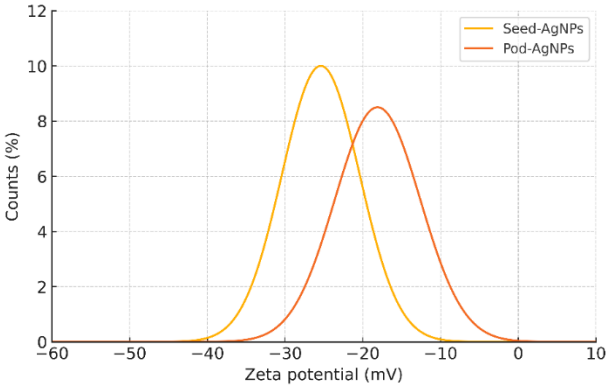

Figure 7. Zeta potential distribution curves of biosynthesized AgNPs. Seed-AgNPs exhibit a zeta potential of −25.4 mV, while Pod-AgNPs show −18.1 mV. These values suggest relatively stable colloidal suspensions, with comparatively higher electrostatic repulsion observed for seed-derived nanoparticles

3.7. Antibacterial activity

The antibacterial activity of the synthesized AgNPs against *Staphylococcus aureus* and *Escherichia coli* is shown in Figures 8 and 9.

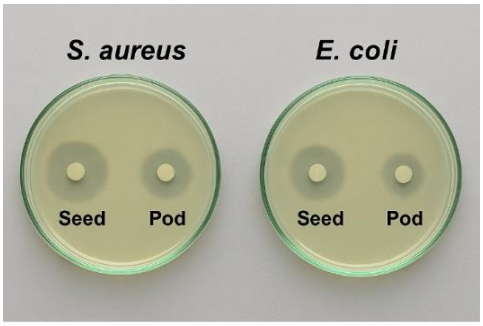

Figure 8. Antibacterial assay plates showing zones of inhibition produced by Seed- and Pod-derived AgNPs against Staphylococcus aureus and Escherichia coli. Clear inhibition zones are observed around the wells, with comparatively larger zones for Seed-AgNPs under the tested conditions.

The concentration-dependent antibacterial responses across 50–200 µg mL⁻¹ are presented in Supplementary Figure S1.Seed-derived AgNPs produced larger zones of inhibition against *S. aureus* (18.2 ± 1.3 mm) and *E. coli* (16.7 ± 1.1 mm) compared with Pod-derived AgNPs (14.1 ± 0.9 mm and 12.9 ± 1.0 mm, respectively). Statistical analysis using one-way ANOVA followed by Tukey's post-hoc test confirmed that these differences were significant (p< 0.01).The magnitude of the differences was further supported by large effect sizes, with Cohen's *d* values of 3.6 for *S. aureus* and 3.2 for *E. coli*, indicating a substantial antibacterial advantage for Seed-AgNPs under the tested conditions. The overall treatment effect was also strong (η^2 = 0.76).Control experiments using crude seed and pod extracts without nanoparticle formation showed only mild antibacterial activity, whereas the water control showed no detectable inhibition (**Supplementary Figure S2B**). These findings suggest that nanoparticle synthesis substantially enhanced antibacterial performance relative to the corresponding crude extracts.This difference may be associated with variations in particle size and colloidal stability. Smaller nanoparticles generally possess a higher surface-area-to-volume ratio, which can enhance their interaction with bacterial cell membranes [13,21]. In addition, improved dispersion stability may facilitate more effective contact between nanoparticles and microbial cells.

Figure 9. Antibacterial activity of Seed- and Pod-derived AgNPs

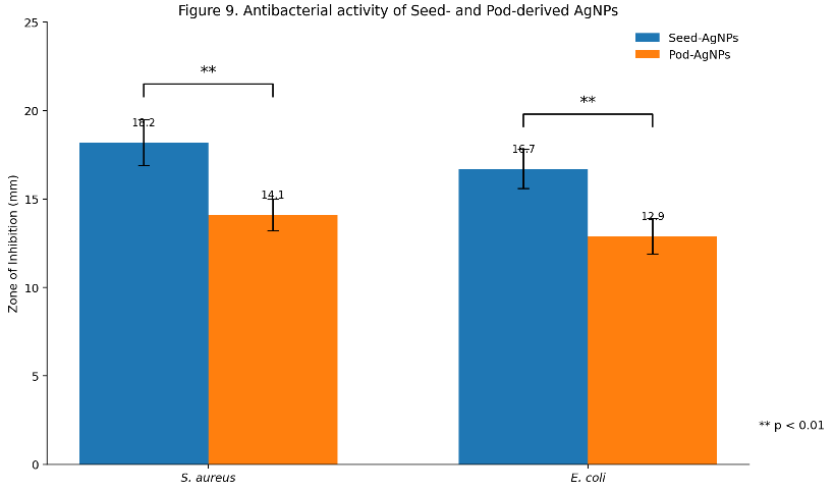

Figure 9. Antibacterial activity of Seed- and Pod-derived AgNPs against Staphylococcus aureus and Escherichia coli. Zone of inhibition values are presented as mean ± standard deviation (n = 3). Error bars represent standard deviation. Statistical significance between Seed- and Pod-derived AgNPs was determined using one-way ANOVA followed by Tukey's post-hoc test (p < 0.01)

Silver nanoparticles are known to exert antibacterial effects through multiple mechanisms, including membrane disruption, protein interaction, and the generation of reactive oxygen species (ROS) [21]. While the present results are consistent with these reported mechanisms, direct measurement of ROS generation or membrane damage was not carried out in this study. Overall, the findings suggest that Seed-AgNPs exhibit comparatively stronger antibacterial activity than Pod-AgNPs under the tested experimental conditions.

3.8. Antioxidant and wound-healing activity

In contrast to the antibacterial results, Pod-derived AgNPs showed comparatively higher antioxidant and wound-healing activity. The DPPH assay indicated greater radical scavenging activity for Pod-AgNPs (81 ± 2.1%) compared with Seed-AgNPs (67 ± 2.4%). Comparative responses of crude extracts and nanoparticle formulations are presented in Supplementary Figure S2A. This difference may be related to variations in surface-associated phytochemicals. Phenolic compounds and tannins are known for their hydrogen-donating and free-radical-scavenging properties, which could contribute to the observed antioxidant activity [12,18]. However, the specific contribution of individual compounds was not directly evaluated in this study.The in vitro scratch assay (Figure 10) showed that Pod-AgNPs were associated with higher wound closure (78 ± 3.1% within 24 h) compared with Seed-AgNPs (55 ± 2.8%). The comparatively higher wound-healing activity of Pod-AgNPs may be associated with the greater phenolic and tannin content of the pod extract, as indicated by the phytochemical analysis. These compounds are reported to possess antioxidant and protective effects that may reduce oxidative stress and create a more favorable

microenvironment for fibroblast survival, migration, and proliferation during wound repair. In addition, the phytochemical capping layer on Pod-AgNPs may influence nanoparticle–cell interactions and support gradual release of biologically active silver species, which could further assist cellular responses involved in tissue regeneration. It is also reported that phenolic-rich systems can help regulate cellular redox balance and support processes involved in tissue repair [22].While the present findings are consistent with such observations, the underlying biological mechanisms were not directly investigated in this study. Overall, the results suggest that pod-derived nanoparticles may be more favourable for antioxidant and wound-healing applications under the tested experimental conditions.

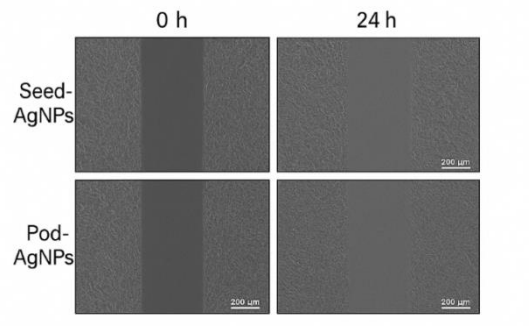

Figure 10. In vitro wound-healing (scratch) assay on human fibroblast monolayers. Representative images at 0 h and 24 h illustrate differences in wound closure, with Pod-AgNPs showing higher closure (~78%) compared to Seed-AgNPs (~55%) under the experimental conditions

3.9. Organ-specific functional divergence

Taken together, the results indicate observable differences in the properties and biological responses of AgNPs synthesized using seed and pod extracts of *A. aromaticum*. Seed-derived nanoparticles were generally smaller, more stable, and showed comparatively higher antibacterial activity under the tested conditions, whereas pod-derived nanoparticles exhibited relatively stronger antioxidant activity and enhanced wound closure in vitro.These differences were observed under identical synthesis conditions, suggesting that variations in extract composition may influence nanoparticle formation and behavior. However, the specific contribution of individual phytochemicals was not directly determined in this study.Overall, the findings highlight that the choice of plant organ can affect the characteristics and observed performance of green-synthesized nanoparticles. Further studies involving detailed phytochemical analysis would be required to establish direct mechanistic relationships.

4. DISCUSSION

The present study examines how organ-specific extract composition within a single medicinal plant may influence the physicochemical characteristics and observed biological responses of silver nanoparticles synthesized under identical conditions. In contrast to many green synthesis studies that focus primarily on nanoparticle formation, this work compares seed and pod extracts of Amomum aromaticum to evaluate potential differences arising from extract source. The results show that Seed-derived AgNPs were smaller in size, exhibited higher crystallinity, and showed greater colloidal stability, along with comparatively stronger antibacterial activity. These observations are consistent with the general understanding that smaller nanoparticles, with higher surface-area-to-volume ratios, can interact more effectively with bacterial cells [13,21]. At the same time, Pod-derived AgNPs, which were relatively larger and likely associated with phenolic-rich surface capping, demonstrated higher antioxidant activity and improved wound closure in vitro. Unlike previously reported cardamom-based nanoparticle systems that commonly relied on a single plant organ, the present dual-organ approach demonstrates complementary functional behaviour within the same species. Seed-derived AgNPs acted as comparatively stronger antibacterial agents, producing a zone of inhibition of 18.2 mm against *Staphylococcus aureus*, whereas Pod-derived AgNPs showed superior antioxidant activity (81 ± 2.1% DPPH scavenging) and enhanced wound closure (78 ± 3.1% after 24 h). These findings suggest that different plant organs may provide distinct phytochemical environments capable of directing nanoparticle properties toward specific biological applications.Since all synthesis conditions were kept constant, the observed differences are likely related, at least in part, to compositional variation between seed and pod extracts. Quantitative phytochemical analysis performed in the present study further supported this view, with seed extract showing higher flavonoid content, while pod extract contained comparatively higher total phenolics and condensed tannins. However, the proposed relationships between specific classes of compounds and nanoparticle behavior should still be considered indicative rather than conclusive.Overall, the findings suggest that plant organ selection may influence nanoparticle characteristics and their apparent biological performance. Further studies incorporating advanced phytochemical profiling, mechanistic investigations, and in vivo validation would be valuable to establish direct causal relationships and broaden potential biomedical applications.

5. CONCLUSION

This study evaluates the use of seed and pod extracts of *Amomum aromaticum* for the green synthesis of silver nanoparticles under controlled conditions. The results show that nanoparticles synthesized from different plant organs exhibit variations in size, stability, and observed biological activity. Seed-derived AgNPs were smaller and more stable, with comparatively higher antibacterial activity, whereas pod-derived AgNPs showed relatively stronger antioxidant activity and enhanced wound closure in vitro.These differences, observed under identical synthesis conditions, suggest that extract composition may influence nanoparticle formation and behavior. However, the specific role of individual phytochemicals was not directly investigated in this study.Overall, the findings indicate that plant organ selection can affect the characteristics and apparent performance of green-synthesized nanoparticles. Further studies involving detailed phytochemical analysis and mechanistic evaluation would be necessary to better understand the underlying processes and potential applications.

Future Aspects

Although the present study suggests that organ-specific extract composition of *Amomum aromaticum* may influence the physicochemical properties and observed biological activity of silver nanoparticles, several aspects remain to be explored in greater detail. Comprehensive phytochemical profiling of seed and pod extracts using techniques such as HPLC, LC–MS, or GC–MS would enable quantitative identification of individual flavonoids, phenolic acids, and tannins, and could help clarify their specific roles in nanoparticle reduction and stabilization. Such analysis would strengthen the mechanistic understanding of the synthesis process. Further optimization of synthesis parameters within each organ-derived system may allow more precise control over nanoparticle size, stability, and dispersion characteristics. In addition, in vivo studies will be important to evaluate biosafety, biodistribution, and therapeutic potential, particularly in the context of wound healing and antimicrobial applications. Finally, extending this organ-specific approach to other medicinal plants with well-characterized phytochemical diversity may provide broader insights into plant-mediated nanoparticle synthesis and its potential applications.

6. REFERENCES

[1] S. Iravani (2011) Green synthesis of metal nanoparticles using plants, *Green Chem.*, 13, 2638–2650, DOI: 10.1039/C1GC15386B.

[2] V. K. Sharma, R. A. Yngard, Y. Lin(2009) Silver nanoparticles: Green synthesis and antimicrobial activities, *Adv. Colloid Interface Sci.*, 145, 83–96, DOI: 10.1016/j.cis.2008.09.002.

[3] M. Rai, A. Yadav, A. Gade (2009) Silver nanoparticles as a new generation of antimicrobials, *Biotechnol. Adv.*, 27, 76–83, DOI: 10.1016/j.biotechadv.2008.09.002.

[4] G. Franci, A. Falanga, S. Galdiero et al. (2015) Silver nanoparticles as potential antibacterial agents, Molecules, 20, 8856–8874, DOI: 10.3390/molecules20058856.

[5] A.-C. Burdușel, O. Gherasim, A. M. Grumezescu et al. (2018) Biomedical applications of silver nanoparticles, Nanomaterials, 8, 681, DOI: 10.3390/nano8090681.

[6] S. Ahmed, M. Ahmad, B. L. Swami, S. Ikram (2016) A review on plants extract mediated synthesis of silver nanoparticles, J. Adv. Res., 7, 17–28, DOI: 10.1016/j.jare.2015.02.007.

[7] V. K. Sharma, J. Filip, R. Zbořil, R. S. Varma (2015) Natural inorganic nanoparticles: formation, fate and toxicity, Chem. Soc. Rev., 44, 8410–8423, DOI: 10.1039/C5CS00236B.

[8] P. Singh, Y. J. Kim, D. Zhang, D. C. Yang (2016) Biological synthesis of nanoparticles, Trends Biotechnol., 34, 588–599, DOI: 10.1016/j.tibtech.2016.02.006.

[9] H. Chugh, D. Sood, I. Chandra, V. Tomar, G. Dhawan, R. Chandra (2021) Role of phytochemicals in nanoparticle synthesis, Mater. Sci. Energy Technol., 4, 1–14, DOI: 10.1016/j.mset.2020.12.003.

[10] A. Roy, O. Bulut, A. K. Mandal, M. D. Yilmaz (2019) Green synthesis of silver nanoparticles, Int. J. Nanomedicine, 14, 7707–7721, DOI: 10.2147/IJN.S214349.

[11] A. Verma, S. Mehata (2016) Controllable synthesis of silver nanoparticles using Neem leaves and their antimicrobial activity, J. Radiat. Res. Appl. Sci., 9, 109–115, DOI: 10.1016/j.jrras.2015.11.001.

[12] B. Balan, M. Supriya, R. Menon (2021) Phenolic compounds in cardamom pods and antioxidant activity, Food Chem., 337, 127776, DOI: 10.1016/j.foodchem.2020.127776.

[13] X. F. Zhang, Z. G. Liu, W. Shen, S. Gurunathan (2016) Silver nanoparticles: synthesis and antibacterial activity, Int. J. Nanomedicine, 11, 5713–5725, DOI: 10.2147/IJN.S121956.

[14] S. Bhattacharjee (2016) DLS and zeta potential – what they are and what they are not, J. Control. Release, 235, 337–351, DOI: 10.1016/j.jconrel.2016.06.017.

[15] T. Wang, X. Lin, Z. Zhang et al. (2018) Silver nanoparticles in wound healing, Nanomedicine, 13, 2537–2554, DOI: 10.2217/nnm-2018-0182.

[16] J. Singh, T. Dutta, K. H. Kim, M. Rawat, P. Samddar, P. Kumar (2018) Green synthesis of metals and their oxide nanoparticles: applications for environmental remediation, J. Nanobiotechnol., 16, 84, DOI: 10.1186/s12951-018-0408-4.

[17] J. Singh, T. Dutta, K. H. Kim et al. (2022) Plant-mediated synthesis of nanoparticles: recent advances, Chemosphere, 286, 134890, DOI: 10.1016/j.chemosphere.2021.134890.

[18] M. Rai, A. Yadav, A. Gade (2008) Current trends in phytosynthesis of metal nanoparticles, Crit. Rev. Biotechnol., 28, 277–284, DOI: 10.1080/07388550802368903.

[19] P. Mukherjee, A. Ahmad, D. Mandal et al. (2001) Bioreduction of AuCl4− ions by the fungus Verticillium sp. and surface trapping of the gold nanoparticles formed, Angew. Chem. Int. Ed., 40, 3585–3588, DOI: 10.1002/1521-3773(20011001)40:19<3585::AID-ANIE3585>3.0.CO;2-K.

[20] R. Narayanan, M. A. El-Sayed (2010) Green synthesis of noble metal nanoparticles using plant extracts and their catalytic applications, Catal. Sci. Technol., 1, 93–102, DOI: 10.1039/C0CY00035D.

[21] Q. L. Feng, J. Wu, G. Q. Chen et al. (2000) A mechanistic study of the antibacterial effect of silver ions on Escherichia coli and Staphylococcus aureus, J. Biomed. Mater. Res., 52, 662–668, DOI: 10.1002/1097-4636(20001215)52:4<662::AID-JBM10>3.0.CO;2-3.

[22] Y. Zhang, H. Chen (2024) Recent progress of silver nanoparticles in wound healing, Mater. Today Bio, 22, 100987, DOI: 10.1016/j.mtbio.2024.100987.

[23] A. Kharissova, H. V. Rasika Dias, B. I. Kharisov, B. O. Pérez, V. M. J. Pérez (2013) The greener synthesis of nanoparticles, Trends Biotechnol., 31, 240–248, DOI: 10.1016/j.tibtech.2013.01.003.

[24] E. A. Ainsworth, K. M. Gillespie (2007) Estimation of total phenolic content and other oxidation substrates in plant tissues using Folin–Ciocalteu reagent, Nature Protocols, 2, 875–877, DOI: 10.1038/nprot.2007.102.

[25] J. Zhishen, T. Mengcheng, W. Jianming (1999) The determination of flavonoid contents in mulberry and their scavenging effects on superoxide radicals, Food Chemistry, 64, 555–559, DOI: 10.1016/S0308-8146(98)00102-2.

[26] P. Schofield, D. M. Mbugua, A. N. Pell (2001) Analysis of condensed tannins: a review, Animal Feed Science and Technology, 91, 21–40, DOI: 10.1016/S0377-8401(01)00228-0.

IZVOD

KOMPARATIVNA ZELENA SINTEZA SREBRNIH NANOČESTICA KORIŠĆENJEM EKSTRAKATA SEMENA I MAHUNA *AMOMUM AROMATICUM* I NJIHOVA BIOLOŠKA PROCENA

Srebrne nanočestice (AgNP) sintetizovane biljnim putem privukle su značajnu pažnju za biomedicinske primene zbog svoje ekološki prihvatljive pripreme, isplativosti i funkcionalnih svojstava. Međutim, većina prethodnih studija koristila je ili jedan biljni organ ili ekstrakte cele biljke, sa ograničenim istraživanjem kako različiti organi iste vrste mogu uticati na formiranje nanočestica i biološke performanse. U ovoj studiji, vodeni ekstrakti semena i mahuna Amomum aromaticum su komparativno korišćeni za zelenu sintezu AgNP pod kontrolisanim uslovima skoro neutralnog spektra (pH 6,0 ± 0,2). Sintetizovane nanočestice su okarakterisane korišćenjem UV-vidljive spektroskopije, FTIR, XRD, TEM, DLS, EDX i analize zeta potencijala. Rezultati su potvrdili formiranje stabilnih i kristalnih AgNP, sa jasnim razlikama u fizičko-hemijskim karakteristikama koje zavise od ekstrakta. AgNP izvedene iz semena bile su manje (15–20 nm) i pokazivale su veću koloidnu stabilnost (−25,4 ± 1,2 mV), dok su AgNP izvedene iz mahuna bile relativno veće (25–30 nm) i pokazivale su različite površinske karakteristike. Biološka procena je pokazala da Seed-AgNP pokazuju relativno jaču antibakterijsku aktivnost protiv Staphylococcus aureus i Escherichia coli, dok su Pod-AgNP pokazale poboljšanu antioksidativnu aktivnost (81 ± 2,1%) i poboljšano zatvaranje rana (78 ± 3,1% u roku od 24 sata) u in vitro testu. Novina ove studije leži u njenom kontrolisanom poređenju specifičnom za organ, pokazujući da različiti delovi iste biljke mogu usmeravati karakteristike nanočestica i funkcionalne odgovore pod identičnim uslovima sinteze. Generalno, nalazi ukazuju da selekcija biljnih organa može značajno uticati na fizičko-hemijska svojstva i posmatrane biološke performanse zeleno sintetizovanih agNP. Potrebna su dalja istraživanja koja uključuju detaljno fitohemijsko profilisanje i mehanističku validaciju kako bi se uspostavile direktne uzročno-posledične veze.

***Ključne reči**: Zelena sinteza; Srebrne nanočestice; Amomumaromaticum; Sinteza posredovana biljkama; Antibakterijska aktivnost; Anti oksidativna aktivnost; Zarastanje rana; Nanobiotehnologija*

Naučni rad
Rad primljen: 29.04.2026.
Rad korigovan: 03.05.2026.
Rad prihvacen: 06.05.2026.

Naveen Pathivada: https://orcid.org/0009-0003-1664-1988
Gopi Mamidi: https://orcid.org/0009-0009-1248-7745
Amancharla Indira Priyadarsini: https://orcid.org/0009-0005-3118-2024
Gunduluru Swathi: https://orcid.org/0009-0005-9008-9532